

The Effect of the Metal Oxidation on the Vacuum Chamber Impedance

Andranik Tsakanian
Hamburg University

Martin Dohlus, Igor Zagorodnov
Deutsches Elektronen-Synchrotron(DESY)

Abstract

The oxidation of the metallic vacuum chamber internal surface is an accompanying process of the chamber fabrication and surface treatment. This circumstance changes the electro dynamical properties of the wall material and as consequence the impedance of the vacuum chamber. In this paper the results of longitudinal impedance for oxidised metallic vacuum chamber is presented. The surface impedance matching technique is used to calculate the vacuum chamber impedances. The loss factor is given for various oxides and oxidation thickness. The numerical results for the undulator vacuum chamber of European XFEL project are presented.

Introduction

The knowledge of the vacuum chamber impedance in accelerators is an important issue to provide the stable operation of the facility from the machine performance and beam physics point of view [1]. The impedances of metallic type vacuum chambers have been studied , for example, in [2-12], including the analytical presentation of the longitudinal and transverse impedances for laminated walls of different materials [8-12] and finite relativistic factor of the particle [11,12]. The metal-dielectric vacuum chamber impedances have been studied in Ref [13-14]. In [14] the longitudinal and transverse impedances for the European XFEL [15] kicker vacuum chamber are calculated based on the field transformation matrix technique [12]. A general approach to evaluate the impedances of the multiplayer vacuum chamber is the field matching technique.

In this paper, the longitudinal impedance of metallic vacuum chamber with internal surface oxidation is studied for ultrarelativistic beam case. The explicit analytical solution is obtained for various thicknesses of the metallic layer and oxidation depth. Based on the obtained results the impedance of European XFEL undulator aluminium vacuum chamber is calculated for various oxidation depths. The explicit analytical solution for longitudinal impedance of two-layer tube is obtained. The exact formula for ultra relativistic point like charge moving on axis is introduced in terms of surface impedance. It is shown that in small oxide depth asymptotic limit the surface impedance on boundary with vacuum can be estimated as a sum of oxide and metal surface impedances. Based on this solution the monopole impedances for aluminium beam pipe with different oxide layer thickness are evaluated.

1. Reflection of electromagnetic fields on boundary of two materials

Plane waves of any polarization can be described as a superposition of waves with perpendicular (TE-mode) and parallel (TM-mode) polarizations to the plane of incident [16, 17]. Let us investigate the reflection of these waves with perpendicular and parallel polarizations (fig.1) for the case when material has finite thickness. The case with infinite wall thickness can be found as a limit. For monopole beam impedance, which will be discussed in next the chapter, only TM-mode is relevant. So in this chapter we will mainly focus on TM-mode.

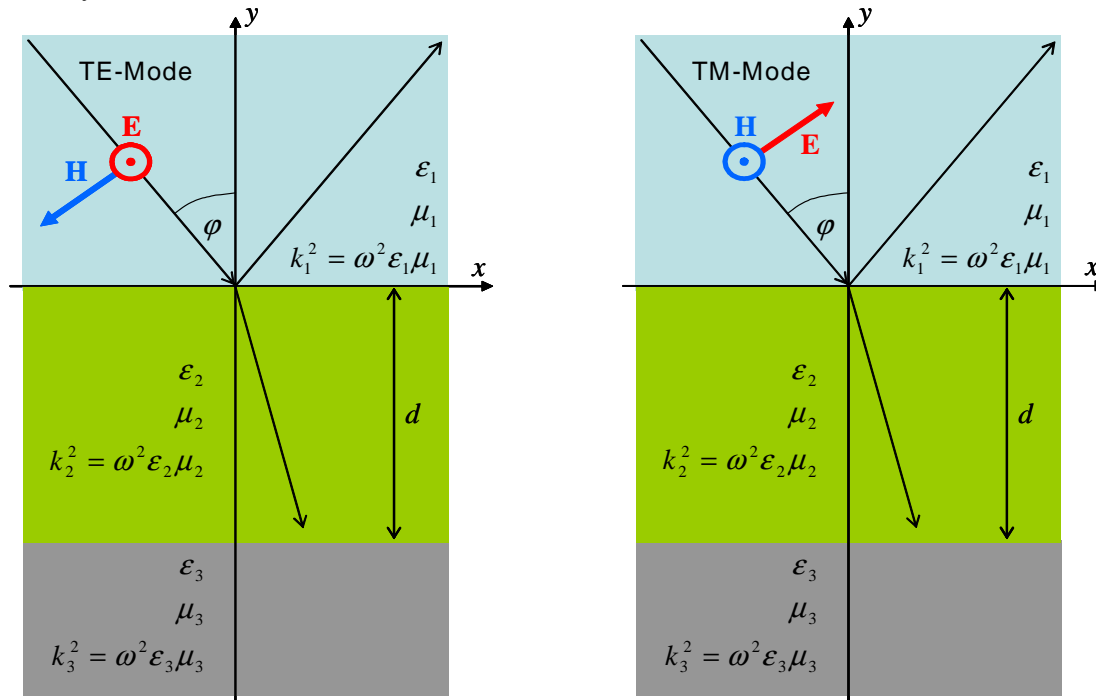


Fig.1 Reflection of plane waves with perpendicular (left) and parallel (right) polarizations from material surface which has finite thickness.

The z-component of magnetic field for TM-mode and the same component of electrical field for TE-mode are

$$\begin{aligned}
 H_{TM,z}^{(1)} &= \exp(-j\vec{k}_1^{in}\vec{r}) - R_{TM} \exp(-j\vec{k}_1^{ref}\vec{r}) \\
 E_{TE,z}^{(1)} &= \exp(-j\vec{k}_1^{in}\vec{r}) + R_{TE} \exp(-j\vec{k}_1^{ref}\vec{r})
 \end{aligned}
 \quad \text{with} \quad \vec{k}_1^{in,ref} = k_1 \begin{pmatrix} \sin \varphi \\ \mp \cos \varphi \end{pmatrix}$$

Where the upper index describe the material number, down index describe the polarization and projection of field.

From Maxwell's equation we get the transverse component of electric and magnetic fields for both kinds of polarizations correspondently

$$E_{TM,x}^{(1)} = \frac{1}{j\omega\epsilon_1} \frac{\partial H_{TM,z}^{(1)}}{\partial y} = \frac{jk_1 \cos \varphi}{j\omega\epsilon_1} \left(\exp(-jk_1^{in} \vec{r}) + R_{TM} \exp(-jk_1^{ref} \vec{r}) \right)$$

$$H_{TE,x}^{(1)} = -\frac{1}{j\omega\mu_1} \frac{\partial E_{TE,z}^{(1)}}{\partial y} = \frac{jk_1 \cos \varphi}{j\omega\epsilon_1} \left(\exp(-jk_1^{in} \vec{r}) - R_{TE} \exp(-jk_1^{ref} \vec{r}) \right)$$

By using the view of field components we can easily find the surface impedance

$$Z_{TM}^{(1)}(\omega, \varphi) = \frac{E_{TM,x}^{(1)}(x, y=0)}{H_{TM,z}^{(1)}(x, y=0)} = \frac{k_1 \cos \varphi}{\omega\epsilon_1} \frac{1 + R_{TM}}{1 - R_{TM}}$$

$$Z_{TE}^{(1)}(\omega, \varphi) = \frac{E_{TE,z}^{(1)}(x, y=0)}{H_{TE,x}^{(1)}(x, y=0)} = \frac{\omega\mu_1}{k_1 \cos \varphi} \frac{1 + R_{TE}}{1 - R_{TE}}$$

Where r_{TM} and r_{TE} are the reflection coefficients. Taking to account the wave vector view $k = \omega\sqrt{\epsilon\mu}$ for surface impedance we get

$$Z_{TM,TE}^{(1)}(\omega, \varphi) = [\cos \varphi]^{\pm 1} \sqrt{\frac{\mu_1}{\epsilon_1}} \frac{1 + R_{TM,TE}}{1 - R_{TM,TE}} \quad (1)$$

The refracted wave field components for TM mode are

$$H_{TM,z}^{(2)} = a_{TM} \exp(-jk_2^{in} \vec{r}) - b_{TM} \exp(-jk_2^{ref} \vec{r})$$

$$E_{TM,x}^{(2)} = \frac{k_{y,2}}{\omega\epsilon_2} \left[a_{TM} \exp(-jk_2^{in} \vec{r}) + b_{TM} \exp(-jk_2^{ref} \vec{r}) \right] \quad \text{with} \quad \vec{k}_2^{in,ref} = \begin{pmatrix} k_{2,x} \\ \mp k_{2,y} \end{pmatrix}$$

And for TE mode

$$E_{TE,z}^{(2)} = a_{TE} \exp(-jk_2^{in} \vec{r}) - b_{TE} \exp(-jk_2^{ref} \vec{r})$$

$$H_{TE,x}^{(2)} = \frac{k_{y,2}}{\omega\mu_2} \left[a_{TE} \exp(-jk_2^{in} \vec{r}) + b_{TE} \exp(-jk_2^{ref} \vec{r}) \right]$$

For surface impedance we get

$$Z_{TM}^{(2a)}(\omega, \varphi) = \frac{E_{TM,x}^{(2)}(x, y=0)}{H_{TM,z}^{(2)}(x, y=0)} = \frac{k_{y,2}}{\omega\epsilon_2} \frac{1 - t_{TM}}{1 + t_{TM}} \quad \text{where} \quad t_{TM,TE} = b_{TM,TE} / a_{TM,TE} \quad (2)$$

$$Z_{TE}^{(2a)}(\omega, \varphi) = \frac{E_{TE,z}^{(2)}(x, y=0)}{H_{TE,x}^{(2)}(x, y=0)} = \frac{\omega\mu_2}{k_{y,2}} \frac{1 - t_{TE}}{1 + t_{TE}}$$

where the upper index (2a) shows the first boundary of second material.

Taking into account the boundary conditions which leads to have continuous tangential component of wave vector

$$k_{x,3} = k_{x,2} = k_{x,1} \equiv k_1 \sin \varphi$$

Using next relation of wave vectors between two medias

$$\frac{k'}{k} = \sqrt{\frac{\varepsilon' \mu'}{\varepsilon \mu}} \quad (3)$$

We can easily find next result

$$Z_{TM}^{(2a)}(\omega, \varphi) = \frac{\sqrt{k_2^2 - k_1^2 \sin^2 \varphi} \frac{1 - t_{TM}}{\omega \varepsilon_2}}{1 + t_{TM}} = \sqrt{\frac{\mu_2}{\varepsilon_2}} \alpha_2 \frac{1 - t_{TM}}{1 + t_{TM}}$$

$$Z_{TE}^{(2a)}(\omega, \varphi) = \frac{\omega \mu_2 \frac{1 - t_{TE}}{\sqrt{k_2^2 - k_1^2 \sin^2 \varphi}}}{1 + t_{TE}} = \sqrt{\frac{\mu_2}{\varepsilon_2}} \frac{1}{\alpha_2} \frac{1 - t_{TE}}{1 + t_{TE}}$$

Where

$$\alpha_2 \equiv \sqrt{1 - \frac{\varepsilon_1 \mu_1}{\varepsilon_2 \mu_2} \sin^2 \varphi}$$

For the second boundary the surface impedance reads

$$Z_{TM,TE}^{(2b)}(\omega, \varphi) = \frac{E_{TM,TE,x}^{(2)}(x, y = -d)}{H_{TM,TE,z}^{(2)}(x, y = -d)} = \sqrt{\frac{\mu_2}{\varepsilon_2}} \alpha_2^{\pm 1} \frac{1 - t_{TM,TE} e^{j2dk_{y,2}}}{1 + t_{TM,TE} e^{j2dk_{y,2}}} \quad (4)$$

For third material the field components for TM mode are

$$H_{TM,z}^{(3)} = g_{TM} \exp(-j \vec{k}_3 \vec{r})$$

$$E_{TM,x}^{(3)} = \frac{1}{j \omega \varepsilon_3} \frac{\partial H_{TM,z}^{(3)}}{\partial y} = g_{TM} \frac{k_{y,3}}{\omega \varepsilon_3} \exp(-j \vec{k}_3 \vec{r}) \quad \text{where} \quad \vec{k}_3 = \begin{pmatrix} k_{3,x} \\ -k_{3,y} \end{pmatrix}$$

And for TE mode we have

$$E_{TE,z}^{(3)} = g_{TE} \exp(-j \vec{k}_3 \vec{r})$$

$$H_{TE,x}^{(3)} = g_{TE} \frac{k_{y,3}}{\omega \mu_3} \exp(-j \vec{k}_3 \vec{r})$$

And for surface impedance we get next result correspondently

$$Z_{TM}^{(3)}(\omega, \varphi) = \frac{E_{TM,x}^{(3)}(x, y = -d)}{H_{TM,z}^{(3)}(x, y = -d)} = \frac{k_{y,3}}{\omega \varepsilon_3} = \frac{\sqrt{k_3^2 - k_1^2 \sin^2 \varphi}}{\omega \varepsilon_3}$$

$$Z_{TE}^{(3)}(\omega, \varphi) = \frac{E_{TE,z}^{(3)}(x, y = -d)}{H_{TE,x}^{(3)}(x, y = -d)} = \frac{\omega \mu_3}{k_{y,3}} = \frac{\omega \mu_3}{\sqrt{k_3^2 - k_1^2 \sin^2 \varphi}}$$

where d is thickness of material. Using next notation

$$\alpha_3 \equiv \sqrt{1 - \frac{\varepsilon_1 \mu_1}{\varepsilon_3 \mu_3} \sin^2 \varphi}$$

and equation (3) we get

$$Z_{TM,TE}^{(3)}(\omega, \varphi) = \sqrt{\frac{\mu_3}{\varepsilon_3}} \alpha_3^{\pm 1} \quad (5)$$

In the case when $|\mu_{2,3} \varepsilon_{2,3}| \gg |\mu_1 \varepsilon_1|$ the $\alpha_{2,3} \approx 1$ approximation is valid. Now by matching the impedances $Z_{TM,TE}^{(3)}(\omega, \varphi)$ with $Z_{TM,TE}^{(2b)}(\omega, \varphi)$ we find the unknown coefficients t_{TM} and t_{TE} correspondently

$$t_{TM,TE} = \frac{1 - A_{TM,TE}}{1 + A_{TM,TE}} e^{-j2dk_{y,2}} \quad \text{where} \quad A_{TM,TE} \equiv \sqrt{\frac{\varepsilon_2}{\mu_2}} \alpha^{\mp 1} Z_{TE}^{(3)}(\omega, \varphi) \quad (6)$$

By matching $Z_{TM,TE}^{(2a)}(\omega, \varphi)$ with $Z_{TM,TE}^{(1)}(\omega, \varphi)$ we find the reflection coefficients for both polarized fields independently

$$R_{TM,TE}(\omega, \varphi) = \left| \frac{u_{TM,TE} - 1}{u_{TM,TE} + 1} \right| \quad \text{with} \quad \begin{aligned} u_{TM} &\equiv \frac{\sqrt{\mu_1 / \varepsilon_1}}{Z_{TM}^{(2a)}(\omega, \varphi)} \cos \varphi \\ u_{TE} &\equiv \frac{Z_{TE}^{(2a)}(\omega, \varphi)}{\sqrt{\mu_1 / \varepsilon_1}} \cos \varphi \end{aligned}$$

In the case when the third material is perfect conductor $Z^{(3)}(\omega, \varphi) \approx 0$ for surface impedance formula is simplified

$$Z_{TM}^{(2a)}(\omega, \varphi) \approx \frac{k_{y,2}}{\omega \varepsilon_2} \tanh(jdk_{y,2}) = j \frac{k_{y,2}}{\omega \varepsilon_2} \tan(dk_{y,2})$$

$$Z_{TE}^{(2a)}(\omega, \varphi) \approx \frac{\omega \mu_2}{k_{y,2}} \tanh(jdk_{y,2}) = j \frac{\omega \mu_2}{k_{y,2}} \tan(dk_{y,2}) \quad (7)$$

Where the y-component of wave vector in second material has the next view

$$k_{y,2} = \omega \sqrt{\varepsilon_2 \mu_2 - \varepsilon_1 \mu_1 \sin^2 \varphi}$$

In thin oxide depth ($d \ll 1$) limit surface impedances will reads

$$Z_{TM}^{(2a)}(\omega, \varphi) \approx j\omega d \frac{\varepsilon_2 \mu_2 - \varepsilon_1 \mu_1 \sin^2 \varphi}{\varepsilon_2}$$

$$Z_{TE}^{(2a)}(\omega, \varphi) \approx j\omega \mu_2 d$$

For non-magnetic materials this formula is simplified

$$\boxed{\begin{aligned} Z_{TM}^{(2a)}(\omega, \varphi) &= j\omega \mu_0 d \frac{\varepsilon_{r,2} - \sin^2 \varphi}{\varepsilon_{r,2}} \\ Z_{TE}^{(2a)}(\omega, \varphi) &= j\omega \mu_0 d \end{aligned}}$$

Where ε_r is relative dielectric permeability. For incident angle $\varphi = \pi/2$ we get

$$Z_{TM}^{(2a)}(\omega, \pi/2) = j\omega \mu_0 d \frac{\varepsilon_{r,2} - 1}{\varepsilon_{r,2}}$$

$$Z_{TE}^{(2a)}(\omega, \pi/2) = j\omega \mu_0 d$$

Let rewrite this equations in next form

$$\boxed{\begin{aligned} Z_{TM}^{(2a)}(\omega, \varphi) &= j\omega L_{TM}(\varphi) & L_{TM} &\equiv \mu_0 d \frac{\varepsilon_{r,2} - \sin^2 \varphi}{\varepsilon_{r,2}} \\ Z_{TE}^{(2a)}(\omega) &= j\omega L_{TE} & L_{TE} &\equiv \mu_0 d \end{aligned}} \quad (8)$$

Since the units of parameters $L_{TM,TE}$ are the same as for inductance, the thin dielectric coating impact on beam impedance can be considered as influence of inductor impedance.

In the case when the third material is not perfect conductor in most practical cases the $|\mu_3 \varepsilon_3| \gg |\mu_1 \varepsilon_1|$ is fulfilled and the surface impedance for both kind of modes are equal and reads as

$$Z_{TM}^{(3)}(\omega) = Z_{TE}^{(3)}(\omega) \equiv Z^{(3)}(\omega) = \sqrt{\frac{\mu_3}{\varepsilon_3}} \approx \sqrt{\frac{j\omega \mu_0}{\kappa(\omega)}}$$

Where $\kappa(\omega) = \frac{\kappa_0}{1 + j\omega\tau}$ is conductivity of conductor with τ - relaxation time.

Taking into account notation in eq.(6) after some manipulations for surface impedance on boundary between vacuum and first material we get

$$\begin{aligned} Z_{TM}^{(2a)}(\omega, \varphi) &= \frac{k_{y,2}}{\omega \epsilon_2} j \tan(dk_{y,2}) + \frac{k_{y,2}}{\omega \epsilon_2} \frac{\tan^2(dk_{y,2}) + 1}{1 + A_{TM} j \tan(dk_{y,2})} A_{TM} \\ Z_{TE}^{(2a)}(\omega, \varphi) &= \frac{\omega \mu_2}{k_{y,2}} j \tan(dk_{y,2}) + \frac{\omega \mu_2}{k_{y,2}} \frac{\tan^2(dk_{y,2}) + 1}{1 + A_{TE} j \tan(dk_{y,2})} A_{TE} \end{aligned} \quad (9)$$

The coefficients $A_{TM,TE}$ we right in next form

$$\begin{aligned} A_{TM} &= \frac{\omega \epsilon_2}{k_{y,2}} Z^{(3)}(\omega) \\ A_{TE} &= \frac{k_{y,2}}{\omega \mu_2} Z^{(3)}(\omega) \end{aligned}$$

For thin dielectric ($d \ll 1$) the asymptotic formula will reads

$$\begin{aligned} Z_{TM}^{(2a)}(\omega, \varphi) &= j\omega \mu_0 d \frac{\epsilon_{r,2} - \sin^2 \varphi}{\epsilon_{r,2}} + \frac{Z^{(3)}(\omega)}{1 + j\omega \epsilon_2 d Z^{(3)}(\omega)} \\ Z_{TE}^{(2a)}(\omega, \varphi) &= j\omega \mu_2 d + \frac{Z^{(3)}(\omega)}{1 + j\omega \frac{\epsilon_2 \mu_2 - \epsilon_1 \mu_1 \sin^2 \varphi}{\mu_2} d} \end{aligned}$$

Finally taking into account notations in eq.(7) and smallness of dielectric layer thickness we get

$$Z_{TM,TE}^{(2a)}(\omega, \varphi) \approx Z_{TM,TE}^L(\omega, \varphi) + Z^\kappa(\omega) \quad (10)$$

Where meaning of the indexes L and κ are inductor and conductor correspondently.

2. Beam Impedance

Consider the relativistic point charge Q moving with speed of light along the z axis of uniform, circular-cylindrical two-layer tube of inner radius R (Fig.2). The charge distribution is then given by $Q(r, \varphi, z) = Q \delta(r) \delta(\varphi) \delta(z - vt)$. The second layer has infinite thickness while the thickness of first one is d .

The cross section of the tube is divided into three concentric regions: 1) $0 \leq r \leq R$ (vacuum), 2) $R \leq r \leq R + d$ (first layer), 3) $R + d \leq r < \infty$ (second layer).

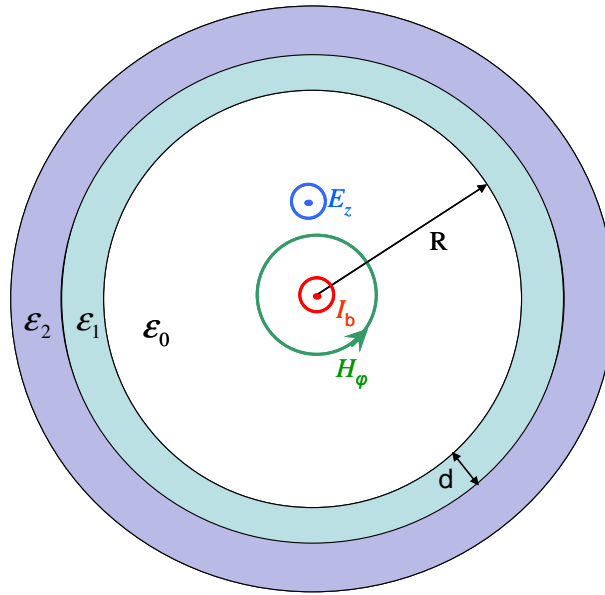


Fig 2. Geometry of the problem

In general, when the charge has non-zero offset, due to current axial asymmetry the fields radiated in the tube have all six components E_z, H_z, E_ϕ, H_ϕ , and E_r, H_r while in particular case when it is on axis only three components are excited E_r, H_ϕ, E_z and they are independent on azimuthal coordinate ref [4]. The Maxwell's equations in frequency domain ($E, H \sim e^{j(z\omega/c - \omega t)}$) for TM mode will reads

$$E_r = Z_0 H_\phi \quad (11.1)$$

$$\frac{1}{r} \frac{\partial(rH_\phi)}{\partial r} = J_z - j\omega\epsilon E_z \quad (11.2)$$

$$jkE_r - \frac{\partial E_z}{\partial r} = j\omega\mu H_\phi \quad (11.3)$$

Where $Z_0 = \frac{1}{c\epsilon_0} = c\mu_0 \approx 377\Omega$ is the impedance of free space.

From equation (11.1) and (11.3) follows that the longitudinal component of electric field is constant

$$\frac{\partial E_z}{\partial r} = 0 \Rightarrow E_z = const \equiv -\frac{A}{j\omega\epsilon_0} \quad (12)$$

Substituting to the second equation we get

$$\frac{1}{r} \frac{\partial(rH_\phi)}{\partial r} = J_z + A$$

Let us rewrite above equation in next form

$$\frac{\partial(rH_\varphi)}{\partial r} = J_z r + Ar \quad (13)$$

Taking into account the relation between current and current density

$$I = \int_S J dS = \iint J r d\varphi dr$$

The integration of equation (13) gives

$$2\pi r H_\varphi = I + A \frac{r^2}{2} 2\pi$$

And for azimuthal component of magnetic field we get

$$H_\varphi = \frac{I}{2\pi r} + A \frac{r}{2}$$

Finally all components of EM field will read

$$\begin{aligned} H_\varphi &= \left[\frac{I}{2\pi r} + A \frac{r}{2} \right] e^{j\left(\frac{\omega}{c}z - \omega t\right)} \\ E_r &= Z_0 \left[\frac{I}{2\pi r} + A \frac{r}{2} \right] e^{j\left(\frac{\omega}{c}z - \omega t\right)} \\ E_z &= -\frac{A}{j\omega\epsilon_0} e^{j\left(\frac{\omega}{c}z - \omega t\right)} \end{aligned} \quad (14)$$

The beam impedance will be

$$Z_b = \frac{E_z}{I} \Big|_{r \rightarrow 0}$$

The unknown coefficient A should be found from boundary condition.

$$Z_s = \frac{E_z}{H_\varphi} \Big|_{r=R}$$

The surface impedance on first boundary could be found using matching technique. In terms of surface impedance for this coefficient it is easy to get following expression

$$A = -j\omega\epsilon_0 I \frac{Z_s}{2\pi R} \cdot \frac{1}{1 + j \frac{\omega R Z_s}{c 2 Z_0}}$$

Finally for beam impedance we get

$$Z_b = \frac{Z_s}{2\pi R} \cdot \frac{1}{1 + j \frac{\omega R Z_s}{c 2 Z_0}}$$

Where surface impedance can be found using the formulas derived in previous chapter where should be taken into account that the electromagnetic field excited by ultra-relativistic charge has only transverse components which leads of $\varphi = \pi/2$ incident angle.

$$Z_s(\omega) \approx Z_s^L(\omega) + Z_s^K(\omega) \quad \text{where} \quad \begin{aligned} Z_s^L(\omega) &= j\omega L & L &= \mu_0 d \frac{\epsilon_r - 1}{\epsilon_r} \\ Z_s^K(\omega) &= \sqrt{\frac{j\omega\mu_0}{\kappa(\omega)}} & \text{with} & \kappa(\omega) = \frac{\kappa_0}{1 + j\omega\tau} \end{aligned}$$

This formula coincides with thin coating asymptotic limit of exact solution for beam impedance of two layer tube derived in ref [10,12].

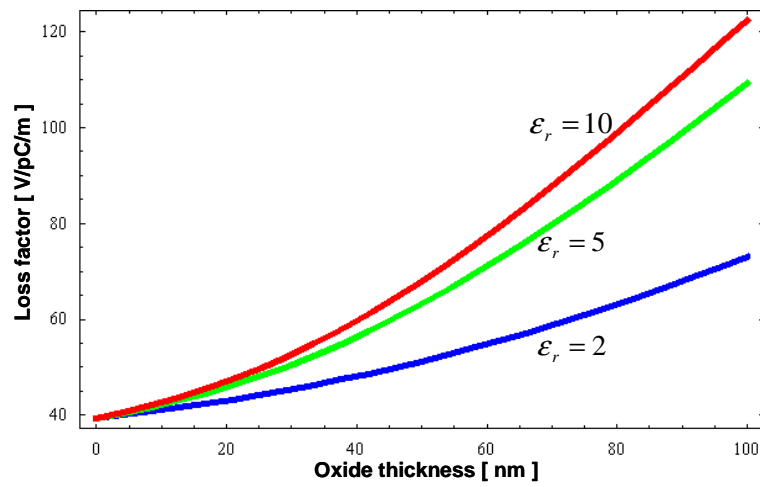
3. Numerical results

In this section we present results of influence of thin oxide layer on loss factor and energy spread. Wake potential of a Gaussian bunch with $\sigma_b = 25\mu m$ rms length was calculated for aluminium ($\kappa_0 = 3.72 \cdot 10^7 \Omega$, $\tau = 7.1 \cdot 10^{-15} s$) beam pipe with 5mm radius. To evaluate loss factor and energy spread next formulas have been used

$$\begin{aligned} \text{Loss factor} &= \langle W \rangle = \int W(s) \lambda(s) ds \\ \text{Energy spread} &= \sqrt{\langle (W - \langle W \rangle)^2 \rangle} = \sqrt{\int (W(s) - \langle W \rangle)^2 \lambda(s) ds} \end{aligned}$$

Where $W(s)$ is a wake potential and $\lambda(s) = \frac{1}{\sqrt{2\pi}\sigma_b} \exp\left(-\frac{s^2}{2\sigma_b^2}\right)$ is a normalized Gaussian distribution function.

a)



b)

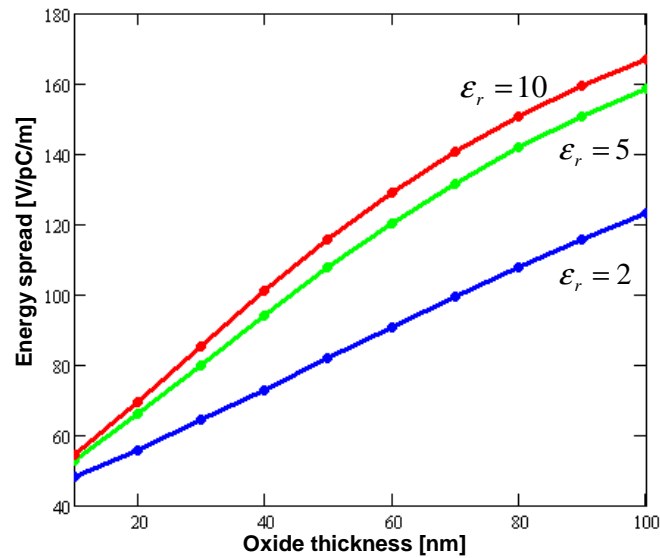
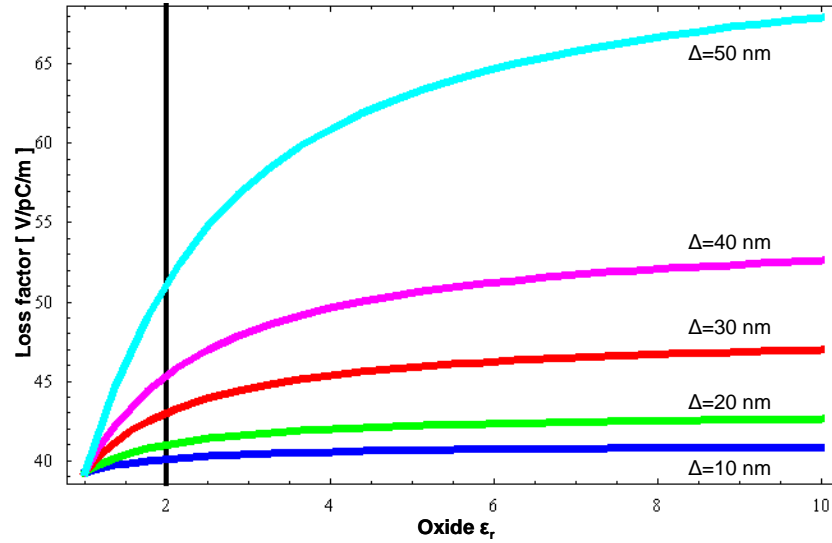


Fig 3. Loss factor and energy spread versus oxide thickness for different kind of oxides.

In figure 3 are plotted loss factor and energy spread versus oxide layer thickness. The calculations are done for three type of oxides with relative dielectric permittivity 2, 5 and 10.

a)



b)

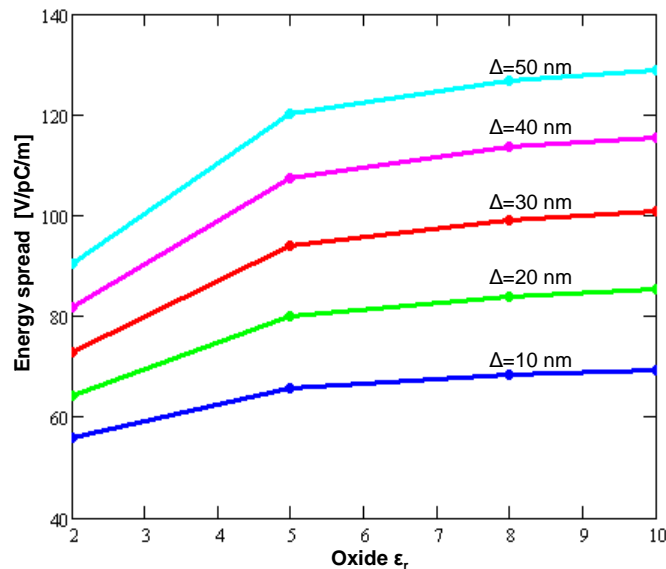
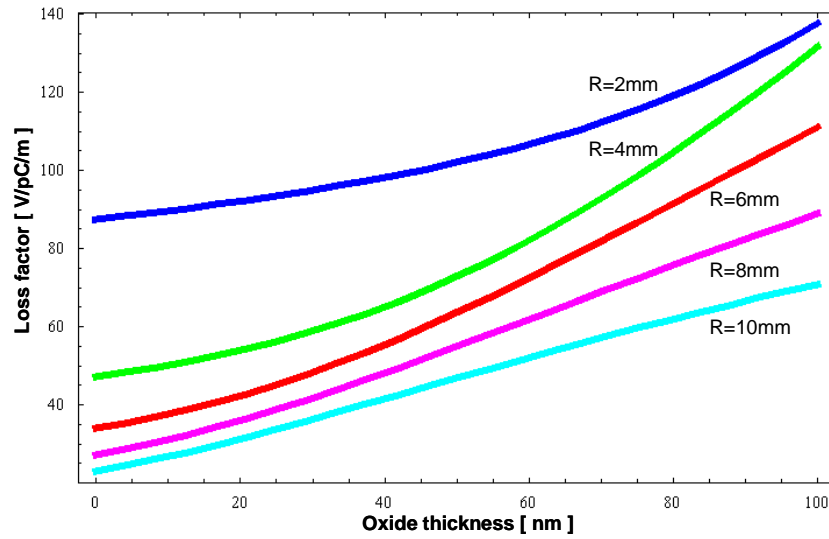


Fig 4. Loss factor and energy spread versus oxide dielectric permittivity for different thickness.

In figure 4 are plotted loss factor and energy spread versus oxide relative dielectric permittivity. As we see from both figures (3, 4) the influence of oxide layer in a worst case when $\epsilon_r = 10$ already at 50 nm thickness increases the loss factors more than 60%.

Since it is unknown the properties and thickness of oxide layer which is appearing during manufacturing of accelerator parts in next figure we make investigation for the worst oxide $\epsilon_r = 10$. In figure 5 is plotted the loss factors versus oxide thickness for different beam pipe radiuses.

a)



b)

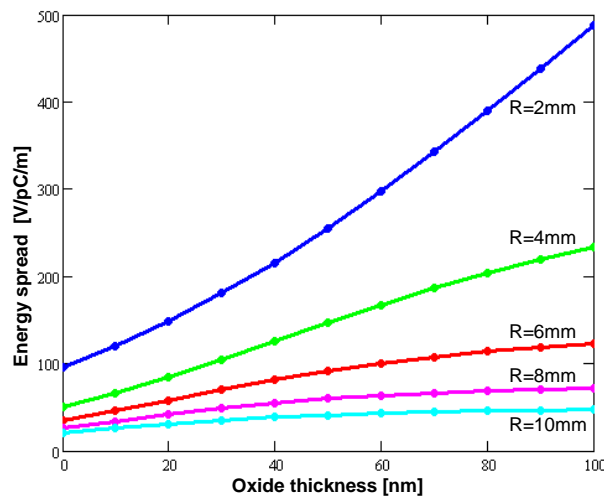


Fig 5. Loss factor and energy spread versus oxide thickness for different beam pipe radiuses.

In European XFEL project the undulator sections are designed with aluminium vacuum chambers with elliptical cross sections. The ellipse diameters in both planes are 15mm and 8.8mm correspondently. Losses in that section can be estimated by round beam pipe model with radius 4.4mm. As we can see from figure 5 already at 60nm oxide thickness the losses increases two times with respect to ideal case (no oxide).

References

1. B.W.Zotter and S.A.Kheifetz, *Impedances and Wakes in High-Energy Particle Accelerators* (World Scientific, Singapore, 1997).
2. H. Henke and O. Napoly, in *Proceedings of the Second European Particle Accelerator Conference, Nice, France, 1990* (Editions Frontiers, Gif-sur-Yvette, 1991), pp. 1046–1048.
3. A. Piwinski, *IEEE Trans. Nucl. Sci.* 24, 1364 (1977).
4. A. Piwinski, Report No. DESY-94-068, 1994, p. 23.
5. A.W. Chao, Technical Report No. 2946, SLAC-PUB, 1982; see also A.W. Chao, *Physics of Collective Beam Instabilities in High Energy Accelerators* (Wiley, New York, 1993).
6. B. Zotter, *Part. Accel.* 1, 311 (1970).
7. D. Jackson, SSCL Report No. SSC-N-110, 1986.
8. M. Ivanyan and V. Tsakanov, *Phys. Rev. ST Accel. Beams* 7, 114402 (2004).
9. A.M. Al-khateeb, R.W. Hasse, O. Boine-Frankenheim, W.M. Daga and I. Hofmann, *Phys. Rev. ST Accel. Beams*, 10, 064401 (2007).
10. M. Ivanyan and V. Tsakanian, *Phys. Rev. ST Accel. Beams*, 9, 034404 (2006).
11. N. Wang and Q. Qin, *Phys. Rev. ST Accel. Beams*, 10, 111003 (2007).
12. M. Ivanyan et al, *Phys.Rev.ST Accel.Beams* 11, 084001 (2008).
13. A. Burov and A. Novokhatskii, INP-Novosibirsk, Report No. 90-28, 1990.
14. A. Tsakanian, M. Ivanyan, J. Rossbach, EPAC08-TUPP076, Jun 24, 2008.
15. M. Altarelli, R. Brinkmann et al (editors), XFEL. The European X-Ray Free-Electron Laser, DESY 2006-097, July 2006.
16. R. E. Collin, “*Foundation for Microwave Engineering*”, McGraw-Hill, 1966.
17. M. Born, E. Wolf, *Principles of Optics*,(1986)